Structure and Interconversion of Oxygen-Vacancy-Related Defects on Amorphous Silica

Chin-Lung Kuo and Gyeong S. Hwang*

Department of Chemical Engineering, University of Texas, Austin, Texas 78713, USA

(Received 28 March 2006; published 8 August 2006)

Atomic structure and structural stability of neutral oxygen vacancies on amorphous silica are investigated using combined Monte Carlo and density functional calculations. We find that, unlike their bulk counterparts, the Si-Si dimer configuration of surface oxygen vacancies is likely to be unstable due to the high tensile strains induced, thereby undergoing thermally activated transformation with a moderate barrier into other stable configurations including dicoordinated silicon, silanone, or a subsurface Si-Si dimer, depending on the local surface structure. Pathways for the interconversion between these oxygen-vacancy-related defects are presented with a discussion of their viability.

DOI: 10.1103/PhysRevLett.97.066101 PACS numbers: 68.35.−p, 61.72.Ji, 68.47.Gh

Pointlike defects may significantly alter the surface properties of amorphous silica (a-SiO$_2$), but their formation, structure, and dynamics are still unclear. In fact, accurate determination of the structure and properties of amorphous oxide surfaces has long been an issue of great importance due to their many applications in electronics, photonics, heterogeneous catalysis, and sensors. However, the difficulty of direct characterization arising from sample charging has impeded progress towards understanding the fundamental behavior and properties of oxide surfaces.

Earlier experimental investigations [1–3] have demonstrated that upon electron irradiation a silica surface undergoes changes in not only photosensitivity but also surface reactivity, mainly due to irradiation-induced defects. Oxygen deficient centers (ODCs) are the most common point defects in oxide materials [4–6]. For silica, oxygen-vacancy-related defects are generally divided into two groups such as paramagnetic and diamagnetic. The paramagnetic E' center comprises an unpaired spin in a sp^3-like orbital of threefold-coordinated silicon (≡Si ·, where the — indicates a Si-O bond). For diamagnetic centers, two different types have been distinguished based on optical absorption and luminescence features, which are commonly denoted as ODC(I) and ODC(II). ODC(I) has been identified as a "relaxed" oxygen vacancy in the dimer configuration (≡Si-Si≡ with the Si-Si bond length of $d_{\text{Si-Si}} \approx 2.46$ Å). While still under controversy, two proposed structural models for ODC(II) include a dicoordinated silicon (=Si:, where the : designates a lone electron pair) [7–9] and an "unrelaxed" oxygen vacancy (with $d_{\text{Si-Si}} \approx 3.1$ Å or $d_{\text{Si-Si}} \approx 4.0$–$4.6$ Å in the pucker configuration) [10]. Previous studies [4,5,11,12] have also suggested the existence of other types of oxygen-deficiency-related centers, such as oxygen divacancy (≡Si-Si-Si≡), Frenkel pair, and silanone group (=Si=O). Recently, optical measurements have suggested photoinduced interconversion between ODC defects in bulk SiO$_2$ [6]. In addition, recent *ab initio* molecular dynamics studies have proposed viable routes for the photoinduced transformation from ≡Si-Si≡ to =Si: or two E' centers ($2E'$) [13,14]. While a great deal of effort has been devoted to understanding the nature of ODCs in bulk SiO$_2$, little is known about the formation, structure, and dynamics of surface defects despite their importance in understanding the complex surface chemistry of a-SiO$_2$.

In this work, we investigated the structure and stability of single oxygen (O) vacancies on the surface of a-SiO$_2$ using combined Monte Carlo and density functional calculations. We first carefully constructed a few model amorphous surfaces that contain a single O vacancy each and then determined O vacancy transformation into other types of point defects. This work represents the first theoretical effort to examine the structural stability and interconversion of ODCs on a-SiO$_2$. The results will contribute greatly to understanding and predicting complex physical and chemical phenomena occurring on the amorphous surface and, in turn, provide a valuable guide for the rational design and fabrication of future silica supported/embedded nanostructure-based devices for various chemical, electronic, and optoelectronic applications.

We constructed defective a-SiO$_2$ surfaces using a combination of METROPOLIS Monte Carlo and first principles density functional calculations. Using the continuous random network (CRN) model [15], we first generated 15 different defect-free bulk structures of amorphous silica at the density of 2.2 g/cm^3. For each structure, we began by placing randomly 120–150 Si and O atoms in a given supercell. The highly strained initial structure was relaxed within the Keating-like model [16] through a series of bond switches using the METROPOLIS Monte Carlo sampling while lowering the temperature from 5000 to 1000 K. We then created an initial surface by inserting a vacuum gap of 10 Å in the z direction for a given periodic supercell. Here all undercoordinated atoms created newly on the bottom surface are terminated by hydrogen atoms. We finally annealed the surface structure using *ab initio* molecular dynamics (MD) within a Born-Oppenheimer framework, followed by static structural optimization. Most of the examined surfaces (with a number of undercoordinated atoms) were well reconstructed within a time scale of

5 picoseconds at 1000 K. During the MD and static calculations, all atoms within a distance of 2 Å from the (H-terminated) bottom surface were fixed to represent the bulk of a-SiO$_2$.

From the calculations, we have identified various surface point defects, including O vacancy ($\equiv$Si-Si$\equiv$), nonbridged O ($\equiv$Si-O), threefold-coordinated Si ($\equiv$Si), silanone group ($=$Si$=$O), and dicoordinated Si ($=$Si:). Since our interest lies in understanding the behavior of O vacancies, among the model surfaces generated, we selected two structures which contain only a single O vacancy each [Figs. 1(a) and 1(c)]. We also constructed an O vacancy by removing a neutral O atom from a defect-free surface [Fig. 1(b)]. Based on the three model surfaces, we examined the structure and stability of single O vacancies at the neutral state on the amorphous surface using density functional calculations.

All atomic structures and energies reported herein were calculated within the generalized gradient approximation (PW91 [17]) to density functional theory using the well established Vienna *ab initio* simulation package (VASP) [18]. A plane-wave basis set for valence electron states and Vanderbilt ultrasoft pseudopotentials for core-electron interactions were employed. A plane-wave cutoff energy of 300 eV was used for *ab initio* MD simulations and 400 eV for static calculations of structure and energetics. The Brillouin zone integration was performed using one k point (at Gamma). The nudged elastic band method (NEBM) was used to determine pathways and barriers for interconversion between oxygen-vacancy-related defects examined. For a given surface structure, maximally localized Wannier functions [19] for weak Si-Si bonds and lone electron pairs associated with defects were also calculated using the CPMD package [20].

Starting from the surface structures, we performed *ab initio* MD simulations at 1000 K. Within a time scale of 3–5 picoseconds, all three surface O vacancies considered were reconfigured from the dimer structure ($\equiv$Si-Si$\equiv$) [(a) in Figs. 2–4] to the puckered structure ($\equiv$Si: + Si$\equiv$) [(b) in Figs. 2–4]. That is, one Si atom of the dimer carries a lone electron pair and the other relaxes backward to interact with a lattice O atom. Then, for each O vacancy we calculated the lowest-energy-barrier pathway for the puckering. The NEBM calculations predict that the reconfiguration would occur with a moderate barrier of 0.4–0.6 eV and an endothermicity of 0.2–0.3 eV.

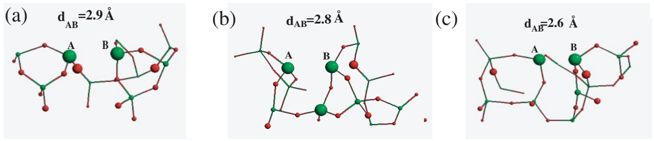

FIG. 1 (color online). Three model surface structures used in this work. Each surface contains an O vacancy in the Si-Si dimer configuration (indicated as A and B). The dimer lengths are given in Å. The lighter (green) and darker (red) colored balls represent Si and O atoms, respectively.

The bistable puckering model has also been proposed for the bulk E' center ($\equiv$Si $\bullet$ +Si$\equiv$) in which the electrophilic Si (Si$\equiv$) moves backward to interact with a lattice O atom [21]. Recent local density functional studies [22] have suggested that the addition of an electron to the E' center fills the dangling bond ($\equiv$Si $\bullet$) rather than the hole (Si$\equiv$), thereby creating a metastable dipole. Unlike on the amorphous surface, the puckered structure turns out to be energetically far less favorable than the dimer structure in bulk a-SiO$_2$; that is, upon capturing an electron, the puckered E' center would transform to the neutral dimer O vacancy with no sizable barrier. We attribute the relative ease of the dimer → pucker reconfiguration on the surface to the surface bonding environment that yields larger tensile strains on the dimer structure. This can also be understood by considering that the bulk generally provides more flexibility in bond rearrangement and, in turn, gives a lower strain energy associated with O vacancies. Indeed, our MD simulation shows that the bond length of surface Si-Si dimers oscillates between 2.6 and 3.1 Å while that of bulk dimers varies from 2.40 to 2.46 Å, indicating that the magnitude of tensile strains exerted on surface O vacancies is generally greater than that on bulk ones. In addition, the sufficient flexibility of the amorphous surface allows puckering to occur even in the absence of a "suitable" back oxygen atom, unlike in the bulk.

Our extensive *ab initio* MD simulations have further demonstrated that the puckered O vacancies are further transformed into other pointlike defects including: dicoordinated Si ($=$Si:), silanone ($=$Si$=$O), and a subsurface Si-Si dimer, as detailed below.

First, as illustrated in Fig. 2, a neutral O vacancy in the puckered configuration [(b)] may convert to a divalent Si defect [(c)] (i.e., $\equiv$Si:Si$\equiv$ → $=$Si: + $=$Si$=$). This transformation would be initiated by the electrostatic interac-

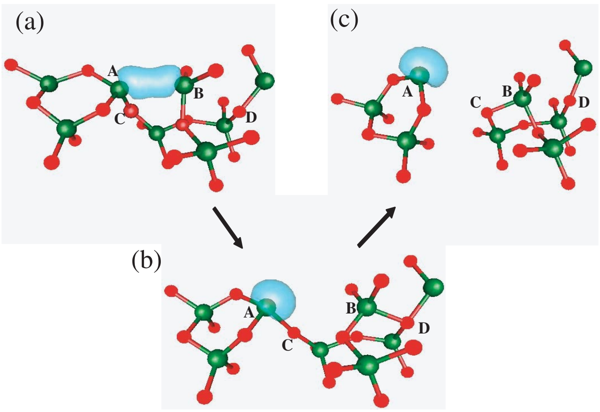

FIG. 2 (color online). Predicted path for the transformation of a surface O vacancy [(a)] to a divalent Si defect [(c)] through a "puckered dimer" structure [(b)]. The isosurfaces of Wannier functions show the presence of a weak Si-Si bond [(a)] and lone electron pairs [(b) and (c)]. The lighter (green) and darker (red) colored balls represent Si and O atoms, respectively.

tion between the electrophilic $\mathrm{Si}\equiv$ (indicated as B) and an (anionic) lattice O [indicated as C, which is initially bonded to the nucleophilic $\equiv\mathrm{Si}$: (A)]. For the model surface considered here, the resulting energy gain and transformation barrier are, respectively, estimated be 1.24 and 0.27 eV. While the relative stability and interconversion barrier can be altered by surface strains, the result suggests the possible creation of stable divalent Si defects from O vacancies on a-$\mathrm{SiO_2}$. We suspect that this transformation may be responsible for thermal desorption of SiO molecules from electron-irradiated a-$\mathrm{SiO_2}$ surfaces where Si content increases as a result of irradiation-induced O desorption [23]. Note that the vacancy-related defect can be healed by SiO desorption, i.e., $\equiv\mathrm{Si\text{-}O\text{-}Si\text{-}O\text{-}Si}\equiv\,\rightarrow\,\equiv\mathrm{Si\text{-}O\text{-}S}\equiv + \mathrm{SiO}(g)$. The details of this reaction will be presented elsewhere.

In fact, the structural conversion from an O vacancy to a divalent Si defect has been proposed to explain photoinduced ODC(I) → ODC(II) transformation in a-$\mathrm{SiO_2}$. While its underlying mechanism is still unclear, a disproportionation-based route [4] has been proposed for the interconversion process. In contrast, our calculation shows that on the amorphous surface the $\equiv\mathrm{Si\text{-}Si}\equiv\,\rightarrow\,=\mathrm{Si}$: transformation can take place via two successive dipole generation/annihilation reactions, i.e., $\equiv\mathrm{Si\text{-}Si}\equiv\,\rightarrow\,\equiv\mathrm{Si}: + \mathrm{Si}\equiv\,\rightarrow\,=\mathrm{Si}: + =\mathrm{Si}=$.

Second, as shown in Fig. 3, a neutral O vacancy in the puckered configuration [(b)] may convert to a divalent Si and silanone pair [(d)]. This transformation involves two steps: (i) a lattice O [indicated as D, which initially bonds to the nucleophilic $\equiv\mathrm{Si}$: (A)] forms a bond with a lattice Si [C, which is the first neighbor of the electrophilic $\mathrm{Si}\equiv$ (B)], which results in a twofold-coordinated Si (A) and a fivefold-coordinated Si (C), i.e., $\equiv\mathrm{Si}: + \mathrm{Si}\equiv + =\mathrm{Si}\equiv\,\rightarrow\,=\mathrm{Si}: + \mathrm{Si}\equiv + \equiv\mathrm{Si}=$, and (ii) the O (E) bonded to the fivefold-coordinated Si reacts with the electrophilic $\mathrm{Si}\equiv$ (B) to create a silanone group, i.e., $=\mathrm{Si}: + \mathrm{Si}\equiv + \equiv\mathrm{Si}=\,\rightarrow\,=\mathrm{Si}: + >\mathrm{Si}{=}\mathrm{O} + =\mathrm{Si}=$. For the model surface considered, the structural reconfiguration turns out to be exothermic by 0.77 eV. This suggests the possible existence of silanone groups on a-$\mathrm{SiO_2}$ through transformation from surface O vacancies.

Indeed, the presence of silanone groups on heavily electron-irradiated $\mathrm{SiO_2}$ surfaces has been proposed to account for the irradiation-induced feature at 91 eV in the Si Auger spectrum [24], while the mechanism for direct silanone group formation is uncertain. Note that electron irradiation commonly leads to creation of a large quantity of O vacancies. In addition, we found that a divalent Si and silanone pair could also be formed via conversion from an epoxide (which was created by removing an O atom from a two-membered ring). Note that the epoxide has been identified as an important point defect on a-$\mathrm{SiO_2}$ [25], but our calculation suggests that it is rather unstable toward structural transformation, particularly when a sizable tensile strain exists along the local surface.

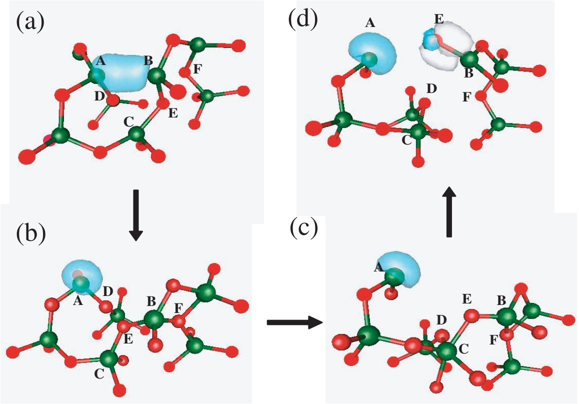

FIG. 3 (color online). Predicted path for the transformation of a surface O vacancy [(a)] to a pair of divalent Si defect and silanone group [(d)] through a "puckered dimer" structure [(b)] and another intermediate state [(c)]. The isosurfaces of Wannier functions show the presence of a weak Si-Si bond [(a)] and lone electron pairs [(b), (c), and (d)]. The lighter (green) and darker (red) colored balls represent Si and O atoms, respectively.

Third, as illustrated in Fig. 4, a surface O vacancy [(a)] may undergo transformation into a subsurface O vacancy in the dimer configuration [(e)] through a divalent Si defect [(c)]. In this case, the dicoordinated Si structure [(c)] turns out to be energetically less favorable than the puckered structure [(b)]. Note that the relative stability between the dicoordinated Si and puckered structures is determined by the surface atomic structure which can vary from site to site on the amorphous surface. Our extensive *ab initio* MD simulations have shown that the rather unstable divalent Si defect easily perishes via three routes, such as: (i) it returns back to the original surface O vacancy; (ii) it converts to another surface O vacancy through a saddle structure of threefold-coordinated O; and (iii) it transforms into a subsurface O vacancy. The transformation from the divalent Si defect to the subsurface O vacancy is likely to follow a two-step mechanism. In the first step [(c) → (d)], the twofold-coordinated Si (B) scavenges a neighboring lattice O (C) which is bonded to a lattice Si (D) in the first subsurface layer. In the model structure considered, this event is predicted to occur by overcoming a barrier of about 0.3 eV. Then, the nucleophilic (B) and electrophilic (D) Si atoms react to form a subsurface Si-Si dimer [(e)], with no sizable barrier. Here, the subsurface O vacancy [(e)] is predicted to be about 1.2 eV more stable than the surface vacancy [(a)]. We also calculated the stability of O vacancies at various locations near the amorphous surface. The result clearly shows that subsurface vacancies are 0.4–1.2 eV more favorable than surface vacancies, due to higher tensile strains associated with the latter.

Based on the first principles calculation results, we could expect that surface O vacancies in the dimer configuration would undergo thermally activated transformation with moderate activation energies into other stable pointlike defects such as divalent Si defects, silanone groups, and/or subsurface Si-Si dimers. The transformation is likely to

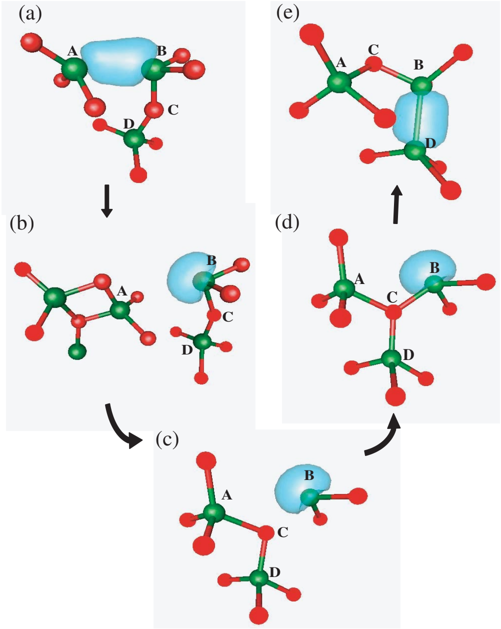

FIG. 4 (color online). Predicted path for the transformation of a surface O vacancy [(a)] to a subsurface vacancy [(e)] through a “puckered dimer“ structure [(b)], a divalent Si defect [(c)], and another intermediate state [(d)]. The isosurfaces of Wannier functions show the presence of a weak Si-Si bond [(a) and (e)] and lone electron pairs [(b), (c), and (d)]. The lighter (green) and darker (red) colored balls represent Si and O atoms, respectively.

be determined largely by the relative stability between the Si-Si dimer and the dicoordinated Si involved, which ultimately depends on the local bonding environment that varies significantly from site to site on the amorphous surface. That is, if the local surface allows stable divalent Si defect formation, a surface Si-Si dimer would prefer transformation into either a dicoordinated Si or a dicoordinated Si and silanone pair, depending on the surface atomic structure. Otherwise, a surface O vacancy is likely to migrate into a subsurface layer. Our results also suggest that the density of O vacancies in the dimer configuration would be minimal on a-SiO$_2$ under thermal equilibrium, unlike other oxide materials such as single-crystalline binary metal oxides where O vacancies play a major role in determining surface properties [26].

In summary, we first constructed three model a-SiO$_2$ surfaces with a single O vacancy each using CRN-based METROPOLIS MC and density functional calculations. Then, based on the model surfaces, we determined the pathways and barriers of the transformation of a surface Si-Si dimer into a dicoordinated Si, a di-oordinated Si and silanone pair, or a subsurface Si-Si dimer using extensive *ab initio* MD and static transition-state search calculations. Our results suggest that surface O vacancies in the dimer configuration would undergo thermally activated transformation with moderate activation energies into other stable pointlike defects including divalent Si defects, silanone groups, and/or subsurface Si-Si dimers. This, in turn, implies that under thermal equilibrium the surface concentration of O vacancies in the dimer configuration would be minimal, while providing a theoretical support for the existence of divalent Si defects and silanone groups on the amorphous surface.

The authors acknowledge the NSF (CAREER-CTS-0449373), the Welch Foundation (F-1535) and the SRC (ID-1292.016) for their financial support of this work.

---

*To whom all correspondence should be addressed.
Electronic address: gshwang@che.utexas.edu

[1] D. R. Allee, C. P. Umbach, and A. N. Broers, J. Vac. Sci. Technol. B **9**, 2838 (1991).
[2] D.-S. Hwang, T. Yasuda, K. Ikuta, S. Yamasaki, and K. Tanaka, Jpn. J. Appl. Phys. **37**, L1087 (1998).
[3] F. Mazen, L. Mollard, T. Baron, S. Decossas, and J. M. Hartmann, Microelectron. Eng. **73–74**, 632 (2004).
[4] G. Pacchioni, L. Skuja, and L. D. Griscom, *Defects in SiO$_2$ and Related Dielectrics: Science and Technology* (Kluwer Academic, Dordrecht, The Netherlands, 2000).
[5] R. A. B. Devine, J.-P Duraud, and E. Dooryhee, *Structure and Imperfections in Amorphous and Crystalline Silicon Dioxide* (Wiley, New York, 2000).
[6] L. Skuja, J. Non-Cryst. Solids **239**, 16 (1998).
[7] A. R. Silin and L. Skuja, J. Non-Cryst. Solids **71**, 443 (1985).
[8] K. Awazu, H. Kawazoe, and K. Muta, J. Appl. Phys. **70**, 69 (1991).
[9] L. Skuja, J. Non-Cryst. Solids **149**, 77 (1992).
[10] H. Imai, K. Arai, H. Imagawa, H. Hosono, and Y. Abe, Phys. Rev. B **38**, 12 772 (1988).
[11] V. M. Bermudez and V. H. Ritz, Phys. Rev. B **20**, 3446 (1979).
[12] G. Pacchioni and G. Ieranò, Phys. Rev. B **56**, 7304 (1997).
[13] T. Uchino, M. Takahashi, and T. Yoko, Phys. Rev. Lett. **86**, 1777 (2001).
[14] D. Donadio, M. Bernasconi, and M. Boero, Phys. Rev. Lett. **87**, 195504 (2001).
[15] F. Wooten, K. Winer, and D. Weaire, Phys. Rev. Lett. **54**, 1392 (1985).
[16] P. Keating, Phys. Rev. **145**, 637 (1966).
[17] J. P. Perdew and Y. Wang, Phys. Rev. B **45**, 13 244 (1992).
[18] G. Kresse and J. Furthmuller, *VASP the Guide* (Vienna University of Technology, Vienna, 2001).
[19] P. L Silvestrelli, N. Marzari, D. Vanderbilt, and M. Parrinello, Solid State Commun. **107**, 7 (1998).
[20] CPMD, Copyright IBM Corporation 1990–2001, Copyright MPI für Festkörperforschung Stuttgart 1997–2004.
[21] M. Boero, A. Pasquarello, J. Sarnthein, and R. Car, Phys. Rev. Lett. **78**, 887 (1997).
[22] Z.-Y. Lu, C. J. Nicklaw, R. D. Schrimpf, and S. T. Pantelides, Phys. Rev. Lett. **89**, 285505 (2002).
[23] S. Fujita, S. Maruno, H. Watanabe, and M. Ichikawa, Appl. Phys. Lett. **69**, 638 (1996).
[24] V. M. Bermudez and V. H. Ritz, Phys. Rev. B **20**, 3446 (1979).
[25] B. B. Stefanov, A. B. Gurevich, M. K. Weldon, K. Raghavachari, and Y. J. Chabal, Phys. Rev. Lett. **81**, 3908 (1998).
[26] C. T. Campbell, Science **299**, 357 (2003).